Towards engineering the design of internal interfaces through interfacial segregation in steels

Mainak Saha[1,2]

[1] Department of Metallurgical and Materials Engineering, National Institute of Technology Durgapur-713209, West Bengal, India

[2]Department of Metallurgical and Materials Engineering, Indian Institute of Technology Madras, Chennai-600036, India

Corresponding authors: Mainak Saha

Email address (es): mainaksaha1995@gmail.com

Phone number: +918017457062

ORCID: Mainak Saha: 0000-0001-8979-457x

Abstract

Several phenomena, including changes in interfacial structure, mobility, cohesion, etc., are caused by soluble decoration at grain boundaries (GBs). Recent experimental studies on interfacial separation in steels are based on the characterization of the microstructure of steels using two correlative methods, namely transmission electron microscopy-atom scanning tomography (APT) and electron backscatter-diffraction-APT. The purpose of this study is to provide an overview of the current state of experimental research in the area of GB segregation in steels, due to the increased interest in this area. Experimental challenges in understanding GB segregation in steel are also highlighted as areas where understanding GB segregation can be useful.

Keywords: Grain boundaries, solute decoration, correlative microscopy, cohesive strength

1. Introduction

Grain boundaries (GBs) are planar (2D) defects that affect the properties of many crystalline metallic materials, including tensile strength. corrosion resistance, duration of hydrogen (H) attack, thermal and electrical conductivity etc. [1]–[5]. The GB can also act as a source and sink of vacancies and dislocations, as it is a region of partial atomic disorder with a defined structure and orientation. [6]–[9]. They also have five macroscopic degrees of freedom (DOF), including misorientation axis and angle. [10]–[15]. The GB structure is determined by five DOFs [16]–[19]. The GB energy, often referred to as the GB energy, is strongly influenced by the GB structure and the chemistry near the GB [17], [18], [20]–[24]. Decreasing the energy of the GB encourages the decoration of the solute in the GB [25]–[27]. Compared with random high-angle GBs (RHAGBs) (with high GB energy), special high-angle GBs (SHAGBs) with low GB energy are said to have higher resistance to corrosion, crack propagation, H -diffusion, GB sliding, etc. [28]–[31]. These observations led to the development of GB Engineering (GBE), which is based on the replacement

of SHAGBs with RHAGBs to optimize properties (of polycrystalline materials). [32]– [37]. However, it is important to consider the effect of primary segregation of different elements (with different concentrations) on GBs [2], [38]-[42]. This is crucial because most GB properties are affected by segregation-induced changes, including fracture strength, electrical and thermal properties, H-embrittlement, resistance to dislocation pile-up, etc. [2], [43]. GBSE separation engineering (GBSE) is the term used to describe this change in GB structure [2]. Co-segregation, separation coefficient and other thermodynamic and kinetic variables such as strain-induced GB phase evolution are all related to GBSE [2] , [44] - [46] . This means that, in addition to thermomechanical processing, time has a significant effect on solute decoration in GBs [2]. In addition, GBSE uses element separation as a site-specific manipulation technique that optimizes the composition and properties of a given GB structure [2]. In addition, the strengths of polycrystalline metallic materials can be reduced or increased by GB [1]. Due to the high stress concentration in GB, most of the used metallic materials are likely to be broken by intergranular fracture due to void nucleation and diffusion [47]. The most typical explanation for such failure is GB-dominant embrittlement caused by plastic strains along the GB that are incompatible in the presence of sequestered solutes [48], [49]. Metallic materials have "reduced ductility" due to this brittle failure [50]. H-separation-induced embrittlement in different GBs of steel is a fairly common example of this phenomenon [2], [51]. Adaptation of plastic stresses along the GB, especially in case of separation of solute, was instead discussed in several articles on the strengthening of GBs (in metallic materials) [40], [52]–[54]. Thus, the main goal is to create metallic materials with high overall durability. The previous remark is often valid in relation to steel, which is the basis of the world economy. In other words, in the design of high quality steels, dissolved decoration can be used at internal interfaces [2]. The purpose of this review is to discuss characterization methods towards understanding GB segregation in steels.

2. Characterising GB segregation in steels

2.1 Common techniques for the characterisation of GB segregation

Several characterisation methods have been used to study GB separation, such as Auger Electron Spectroscopy (AES), Transmission Electron Microscopy (TEM), Scanning Transmission Electron Microscopy (STEM), Electron Backscatter Diffraction (EBSD), Transmission Kikuchi Diffraction (TKD), Electron Energy Loss Spectroscopy (EELS), Field Ion Microscopy (FIM), secondary ion mass spectroscopy (SIMS) and atom probe tomography (APT). When used alone to characterize GB segregation, all these methods have several disadvantages, mainly the lack of crystallographic information and high spatial resolution data [2]. Furthermore, since GB segregation occurs at the atomic scale, it is difficult to simultaneously collect accurate, statistically significant, and reproducible data on GB segregation [2]. Wynblatt and Chatain highlighted the current gap

between theoretical and experimental approaches to combat GB segregation [82]. Correlative microscopy, which allows simultaneous determination of both structural and chemical information of the surrounding region of a solute-decorated GB, is one of the recently developed approaches to characterize GB segregation. The two correlative characterization methods used (so far) to evaluate GB segregation in steels are based on direct lattice reconstruction of APT data of solute-decorated GBs (correlative TEM-APT and EBSD-APT approaches) [2], [83] -[85] . In addition, many factors can influence the GB segregation data obtained by electron microscopy techniques such as TEM and EBSD. First, the angular resolution of the electron microscopy method used must be taken into account. Depending on the instrument and analysis software used, an angular resolution of 1° can be achieved using TEM-based nanobeam diffraction compared to that achieved by the EBSD technique (1–3°) [86]. Second, the use of a focused ion beam (FIB)-based lift-off process to produce APT tips (including the GB region) in a scanning electron microscope (SEM) is full of ambiguity [2], [87]. In the past, orientation mapping of APT tips using TEM and/or FIM techniques has been used to alleviate this problem. In addition to the limited field of view, using these approaches requires a high level of expertise to obtain accurate orientation information (from APT indications). The field of view of the TKD technique is greater than that of the TEM and FIM procedures [88, [89]. Additionally, TKD is significantly easier to use than TEM and/or FIM procedures to obtain orientational information [90]. The effect of projection and lensing on the distribution of atoms for a given GB [91]–[93] is one of the limitations of APT. The lens effect is related to field evaporation in solute-decorated GBs and causes inaccuracies in field localization evaporated atoms, while the projection effect is based on the magnetic field around the APT tip [91].

2.1.1 Conventional methodology

Grabke et al. [94] studied the segregation of Ti, Nb, Mo and V and related carbides in RHAGBs in Fe-P-based ternary and quaternary alloys (bulk composition defined in reference [94]) using FIM, APT and AES techniques. In Fe-Ti-P steel alloys, the addition of Ti and Nb has been shown to prevent the release of P in GB (through the creation of Ti- and Nb-based phosphides) [94]. However, it was found that neither Mo nor V affected the tendency of P to segregate [94]. P GB segregation in Fe-Nb-C-P and Fe-Ti-C-P quaternary alloys increases with C content until NbC is precipitated [94]. Christie et al. [95] showed a linear relationship between the P content sequestered in GBs of 17-4PH martensitic stainless steel and intergranular grooves formed during metallographic etching. Takahashi studied the separation of C and N atoms in different GBs in Fe-0.006C-0.001N-0.04Al (C60) and Fe-0.005C-0.0054N-0.04Al (N60) (wt%) steels in ferritic et al. . . . . [96] using APT. It has been noted that, based on observations, C is released in RHAGBs at C60, while N is released at N60 in RHAGBs [96]. However, it was shown that N had a lower tendency to release in N60 than C

in C60 [96]. In addition, segregation of C atoms in RHAGBs (in C60), rather than segregation of N atoms in RHAGBs (in N60), was found to affect the Hall-Petch coefficient of ferrite grains [96]. Rosa et al. [97] used nano-SIMS and APT techniques to investigate the effects of B addition on high-strength Fe-0.34C-2.45Mn-0.0100B-0.03Ti (at. %) steel (with single-phase austenite structure). The release of B in RHAGB is due to the dissolution of boride (Fe2B and M23(B,C)6) within the grain [97]. In addition, the degree of B segregation in austenitic GBs was found to increase with increasing temperature [97]. B segregation in austenitic GB was suggested to follow a Langmuir–McLean adsorption isotherm [97], despite this contradicting the thermodynamically supported trend of decreasing solute segregation with increasing temperature. B segregation has been argued to follow a Langmuir–McLean adsorption isotherm [97] despite the fact that this contradicts the thermodynamically supported trend that solute segregation decreases with increasing temperature. Based on this isotherm, the enthalpy of dissolution of borides (ΔHdiss) and ΔHi B (with austenitic GB) was calculated to be higher (51% and 9.4%, respectively) than the corresponding values (ΔHi and ΔHdiss) published in previous literature [98]–[100]. Using APT, AES and fractography techniques, Fedotova et al. [101] investigated radiation-induced segregation of P, Mn, Ni and Si GBs in RHAGBs Fe-(0.04–0.07)C-(1.6–1.89)Ni-(0.006–0.01)P (wt.%) in ship steels at reactor pressure The degree of separation of these elements (in RHAGBs) has been reported to increase with large concentration [101]. In addition, P segregation was found to promote intergranular fractures in RHAGB [101]. Similar P trends were observed in neutron-irradiated AISI 304 austenitic stainless steel [103], [104] and Fe-(0.083–0.19)C-(0.26–0.38)Si-(1.22–1, 41)Mn-(0.007). -) 0.012 P (wt%) reactor pressure vessel steels. Using aberration-corrected STEM ANGELS, Shigesato et al. [105] investigated the non-equilibrium segregation of B in austenitic RHAGBs in Fe-0.05C-0.5Mo-0.001B (wt%) steel. In addition, this work [105] evaluated the effects of sample thickness, electron beam broadening and GB plane orientation on B GB segregation. The broadening of the B concentration profile was calculated using the Gaussian broadening model [105]. The thickness of the sample increases the degree of expansion [105]. Broadening of the B concentration profile was found to be 10% for a sample thickness of 30 nm [105]. In addition, the B concentration profile was found to be asymmetric for GB plane tilt angles greater than 1.5° [105]. In a duplex environment, Mn steel (composition: Fe-11.7Mn-2.9Al-0.064C (wt%)) Ma et al. [106] showed that the release of C at the ferrite/austenite interface (IB) increases the dislocation emission energy barrier of RHAGBs, leading to intermittent release of the material at room temperature. It has been suggested that discontinuous yielding phenomena are affected by the C decoration in the aforementioned IB with dislocation nucleation and subsequent propagation [106] . Furthermore, contrary to previous results [107]–[109] , Gibbs and Langmuir-McLean adsorption isotherms were shown not to be responsible for solute separation in IBs.

2.1.2 Correlative methodology

TEM-APT methodology

Herbig et al. [86] characterized C-decorated GBs of nanocrystalline cold-drawn pearlite steel (composition: Fe-4.40C-0.30Mn-0.39Si-0.21Cr (at. %)) using correlative TEM-APT methodology and reported C excess (obtained using APT) as a function of GB misorientation angle for coherent Σ5 and both coherent and incoherent Σ3 GBs (Fig. 1). The overlap of C decoration in different GBs of the APT needle is shown in Fig. 1 (a). The variation of C excess as a function of GB error angle is shown in Fig. 1(b). The C excess was found to be significantly higher for incoherent Σ3 GBs than for coherent Σ5 and Σ3 GBs [86]. In addition, the appearance of inappropriate dislocations, which is also responsible for the significant C excess in the mentioned GB (Fig. 1 (b)), was found to be due to the deviation from the optimal 60° misorientation (in case of incoherence). 3 GB) [86]. For the aforementioned GBs, it was also shown that excess C vs. The GB misorientation angle plot had a strong relationship with the GB energy versus misorientation angle plot [86]. A similar methodology was used by Abramova et al. [110] show how the segregation of Mo, Si and Cr in austenitic RHAGB leads to GB strengthening in ultrafine grain AISI 316 austenitic stainless steel. Han et al. [111], using the above technique, reported that the competitive separation of C and P (in RHAGBs) significantly affects the delamination of ferritic steel. In addition, high P and low C RHAGBs were found to induce delamination cracks, while low P and high C RHAGBs were found to be resistant to delamination cracks [111].

.

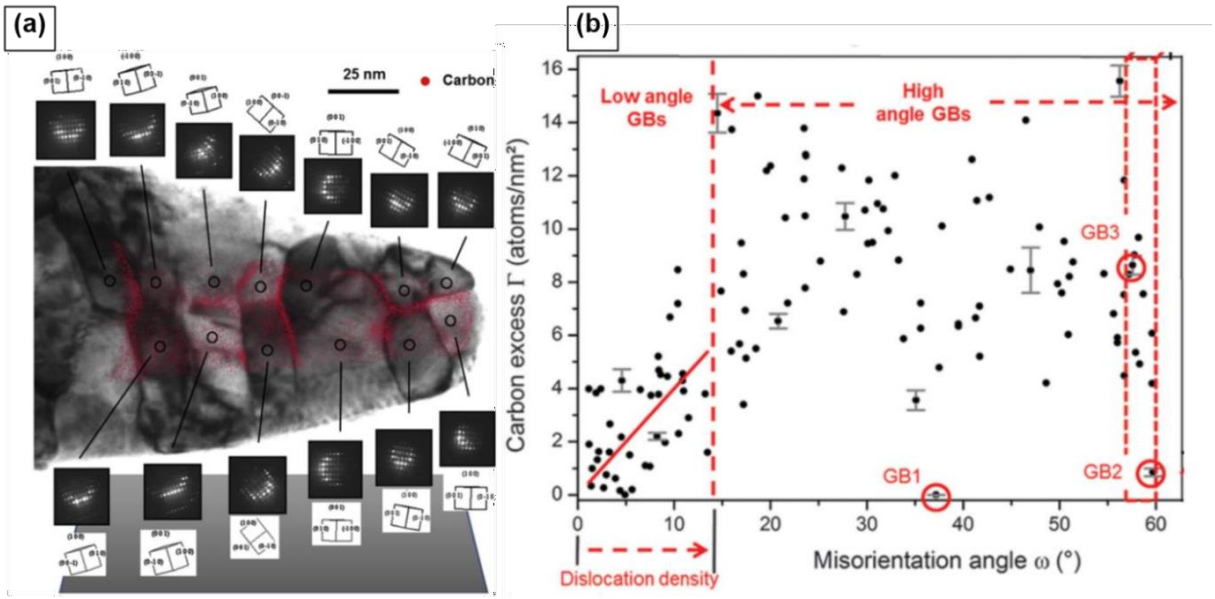

Fig. 1 Correlative TEM-APT analysis for cold drawn pearlitic steel with the following composition: Fe-4.40C-0.30Mn-0.39Si-0.21Cr: APT needle prepared using FIB-based liftout approach (a) Overlay of C decoration at various GBs (b) Variation of C excess as a function of

GB misorientation angle [86].

EBSD-APT methodology

This method was used by Kuzmina et al. [112] show how Mn segregation causes embrittlement of martensitic RHAGBs in Fe-9Mn-0.05C (wt%) steel at 450 °C. in In this situation, it was reported that the addition of 0.0027 wt% B strengthened the GB and prevented the release of Mn in martensite in RHAGB, promoting the return of martensite to austenite at a longer holding of about 336 h at 450 °C. [112] Benzing et al. [113] found a similar observation for Fe-12Mn-3Al-0.05C (wt%) steel. This method was used by Ravi et al. [114] to investigate the effect of C segregation in Fe-0.2C-3Mn-2Si (wt%) bainitic steel. They found that C segregation in austenitic RHAGBs facilitates austenite to bainite transformation at isothermal transformation temperature (400 °C in this case). Herbig et al. characterized the segregation of B, C, P, Si and Cu in FCC RHAGB and coherent Σ3 annealing twin boundary Fe-28Mn-0.3C (wt%) twin-induced plasticity (TWIP) steel. [115] using the same method (Fig. 3).

Addition of C atoms to RHAGB (Fig. 2) is reported to increase the local stacking fault energy (SFE), which in turn induced a large resolved shear stress for mechanical twinning (in RHAGB) [115]. On the other hand, depletion of C (Σ3 with Gt; Fig. 2(c)) was found to reduce the local SFE and lead to the development of the ε-martensite (HCP) phase at the austenite Σ3 boundaries [115] . In addition, it was investigated whether elements (B, C, P, and Si) were preferentially segregated during deformation and/or annealing in doubly deformed Fe-22Mn-0.6C (wt%) TWIP steel [115]. Although deformed twins have identical crystal structures, their propensity for C atom decoration is significantly lower than that of annealed twins [115]. The very poor mobility of C atoms in the production of deformation twins at room temperature may be the reason for this deformation twin tendency [115].

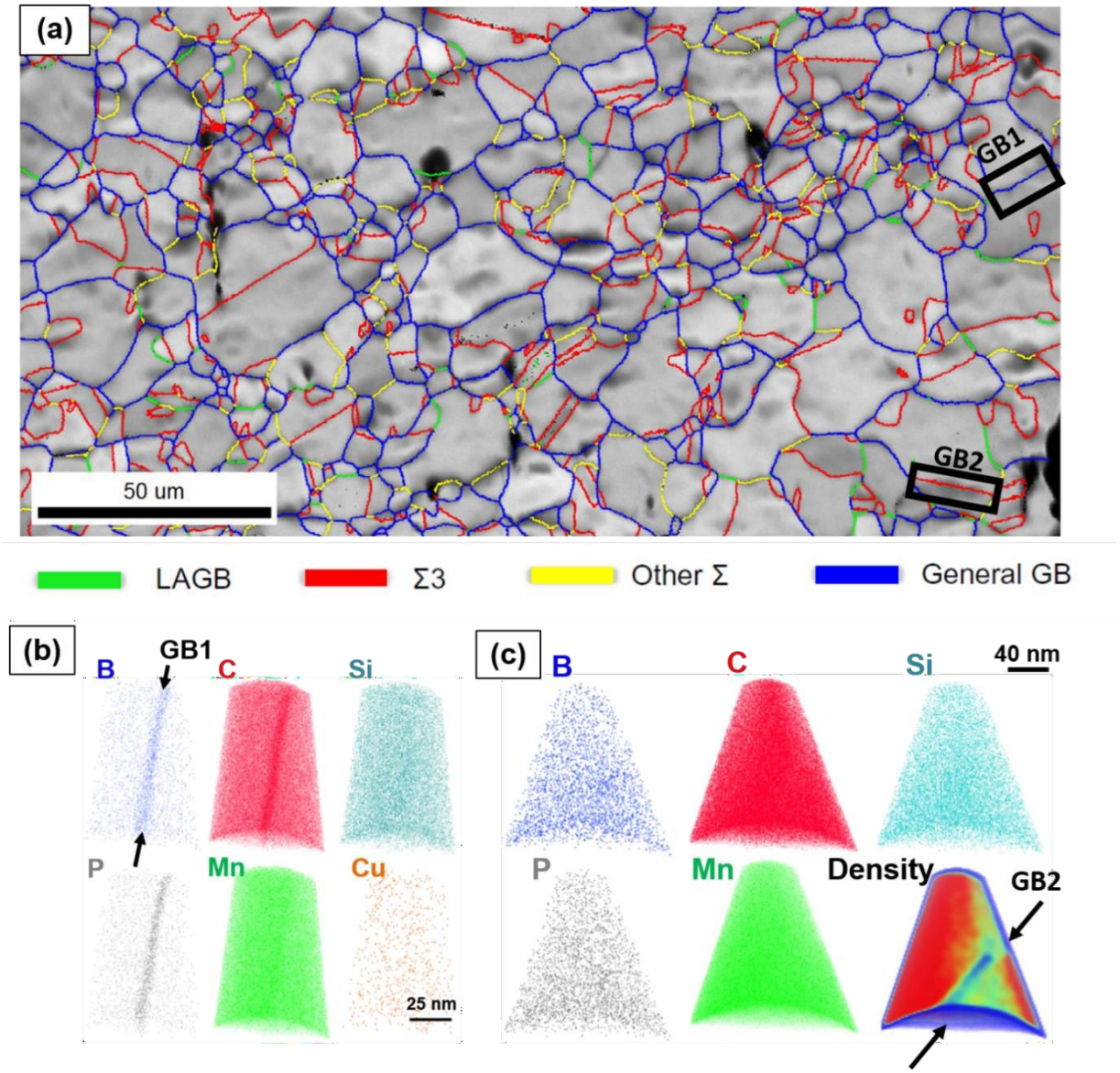

Fig. 2 Correlative EBSD-APT analysis for Fe–28Mn–0.3C (wt.%) TWIP steel: **(a)** EBSD-based IQ+GB map showing the two GBs: GB1 and GB2 (enclosed in black outlined rectangular boxes) analysed using APT, APT-based 3D elemental maps for different elements in **(b)** GB1 and **(c)** GB2. In part **(a),** LAGB abbreviates for low-angle grain boundary and general GB refers to RHAGB. To the bottom right of part **(c)**, Density map (of Fe) shows the position of GB2 [115].

Araki et al. [116] developed a systematic correlation between the critical shear stress of GB dislocation emission and C (a) concentration within the grain and (b) RHAGB concentration in Fe-50C (ppm) ferritic steel using the aforementioned correlation method with nanoindentation. technique Based on this study, it was found that (i) the generation and propagation of dislocations occurs much more easily in the RHAGB than in the grain interior due to the high frequency of "pop-in events" (in the load-displacement curves) in the RHAGB and (ii) dislocation pinning at RHAGB caused by C atoms results in a high critical shear stress for dislocation emission in RHAGB, leading to GB strengthening [116]. In addition, before the onset of "pop-in events" in the nanoindenter-based load-displacement curves, the

critical shear stress required for displacement of the RHAGB was estimated using Hertzian contact theory, considering the elastic contact between the nanoindenter and the sample surface [116].

2.4. Towards utilising GB segregation: Examples

2.4.1 Alloy design

One application of GB segregation in steel construction is to stabilize nano-sized grains by reducing the total energy of GBs through the decoration of GB solutes. For example, discontinuous grain growth (due to high GB energy) is a common phenomenon in many materials, especially steels. In this situation, the GB allocation is useful in two different ways. This first lowers the GB energy and then the capillary force associated with the competitive growth of two adjacent grains. Second, the selection of appropriate solutes (for decoration in GBs) improves the cohesive strength of GBs. Yuan et al. [117], the release of C in martensitic GBs increases the tensile strength and total elongation (about 233.33% and 53%, respectively) for Fe-13.6 Cr-0.44 C (wt%) martensitic steel. This is explained by the separation of C in the martensitic GBs, which favors the transition from the martensite to the austenite phase [117]. Fe-3.66C-0.48Mn-0.39Si-0.01P-0.01S (at.%) in pearlitic steel Li et al. [118] found a direct relationship between the amount of tensile stress and the concentration of separated C in ferrite RHAGBs. In addition, the hypereutectoid Fe-4.40C-0.30Mn-0.39Si-0.21Cr-0.003Cu-0.01P-0.01S (at.%) in the pearlitic steel has a similar correlation with the C situation in the sub-steel. isolated ferrite (or , low-angle) boundaries are presented in [119], [120]. The design of H-hardening (HE) steels is another application where knowledge of GB segregation can be useful. One of the common problems in automotive steels is HE [121]–[129]. Since H is the smallest atom (atomic radius 0.037 nm), it easily diffuses into materials (especially steels) and causes catastrophic and unprecedented failures of technical components in use [122]. In addition, it is difficult to map the exact location of H in the material due to the exceptionally high atomic mobility of H (due to the small atomic radius). Therefore, it is very difficult to validate several existing tactics (developed for steels such as carbide addition). Chen et al. [124] recently established a deuterium charge-based cryotransfer process to locate H atoms at different GB points in Fe-0.23C-0.92Mn-0.24Si-0.049Nb (wt%) steel using characterization techniques such as TEM, TKD, and cryo-APT. Two different microstructures were investigated with this technique: fully martensitic and fully ferritic [124]. Deuterium has been shown to be released at incoherent interfaces between NbC and ferrite in a fully ferritic microstructure and between NbC and martensite rows in a fully martensite microstructure [124] . This was the first experimental observation of carbide's ability to hold hydrogen atoms. It was also found that for a fully martensitic microstructure, C segregates significantly at the low-angle boundary [124]. It has been shown

that C is essentially sequestered in ferrite RHAGBs with a fully ferrite microstructure [124]. In addition, the GB defect angle in ferrite RHAGBs was found to affect the GB segregation tendency of C atoms [124]. In both microstructures, simultaneous segregation of both C and H atoms (at different GBs) was observed [124]. Despite the high affinity of C for the H atom, H has been reported to be trapped in the GBs [124].

2.4.2 Stress and segregation-induced phase transformation at a GB

Raabe et al. [2], local elastic stresses and solute element decoration (GB) can be used to promote the local phase transition. This is often observed when martensite to austenite transformation occurs in martensitic GBs. The GB energy of martensite affects the reverse phenomenon [130]. In addition, it was found that the transformed region (in GBs) can absorb local elastic stresses, leading to a local transformation-induced plasticity effect (TRIP) in transformed austenitic GBs, which facilitates further phase transformation [120], [130] . The martensite phase shape significantly affects the martensite GB energy [49]. For example, different types of martensitic GBs such as lath, needle and packet boundaries have been reported in the literature [2], [119]. Of all these limits, the lattice limits are the least associated with the GB energy [2], [131]–[134]. The above-mentioned reverse is said to be a very successful technique to stop intergranular fractures propagating along martensitic GBs. However, several criteria for this recovery to occur have been documented in the current literature [135]–[138] . First, it is necessary to select solutes with high β_i [138]. Second, martensitic GBs are preferred to experience preferential separation of solute species [49]. Third, solutes should be more likely to disperse in GBs than precipitates (for example, many transition elements such as Ti, V, Cr, Nb, etc. form carbides) [49]. Fourth, the separated solutes must lower the temperature at which martensite transforms into austenite [135], [136]. Furthermore, strengthening in GBs must be facilitated by austenite nucleation in GBs [2], [5] and associated local elastic stresses [137].

3 Future directions

Addressing all five macroscopic and three microscopic DOFs (associated with GBs) is an important topic for GB studies. Despite the fact that the 3D EBSD technique (proposed in Ref. [138]) addresses all five DOFs (in GBs), the three microscopic DOFs have not yet been addressed experimentally. In addition, the 3D EBSD approach requires an additional FIB setup in the SEM and is quite time consuming. Therefore, this characterization cannot be done by conventional SEM, unlike the conventional 2D-EBSD method. The limitations of combining GB structure and dissolved decorations with its general effect on material mechanical performance stem from the inability to handle eight DOFs. However, only the degree of GB segregation is required when using GB segregation data to minimize the total grain size. Extensive 5D GB analysis is not necessary in this case, as the GB level information can be ignored [2]. In addition, 3D-EBSD uses

serial shear, which makes it potentially harmful [138], [139]. In other words, since the region under study is already lost in 3D-EBSD mapping and is not available for APT analysis, it is not possible to develop a correlative 3D-EBSD-APT methodology to obtain both structural and chemical information from the same region. . in microstructure [139]. However, it is there is currently a lack of knowledge about how the density of different solute species and the dislocation density (in stacks near GBs) affect the cohesive strength of GBs. This may be due to several experimental difficulties in elucidating how GB interacts with decorative solutes. It may be possible to use a correlative approach of microstructural characterization together with relevant theoretical studies to solve the above problem.

4 Summary and conclusions

There are several phenomena that often result from solvent decoration at internal interfaces, such as stress-induced phase transformation (at internal interfaces), phase growth, phase recovery, and intergranular embrittlement. From a metallurgical perspective, interface separation can be used to chemically and structurally manipulate internal interfaces. The main purpose of this change is to improve the general mechanical performance of the steels. However, correlative microscopy can be used as a tool for the production of high-strength steel with appropriate theoretical justifications.

References

[1] M. P. Seah, “Interface adsorption, embrittlement and fracture in metallurgy. A review,” *Surface Science*, vol. 53, no. 1. pp. 168–212, 1975. doi: 10.1016/0039-6028(75)90124-7.

[2] D. Raabe *et al.*, “Grain boundary segregation engineering in metallic alloys: A pathway to the design of interfaces,” *Current Opinion in Solid State and Materials Science*, vol. 18, no. 4. Elsevier Ltd, pp. 253–261, Aug. 01, 2014. doi: 10.1016/j.cossms.2014.06.002.

[3] C.-S. Kim, Y. Hu, G. S. Rohrer, and V. Randle, “Five-parameter grain boundary distribution in grain boundary engineered brass,” *Elsevier*, doi: 10.1016/j.scriptamat.2004.11.025.

[4] C. A. Schuh and K. Lu, “Stability of nanocrystalline metals: The role of grain-boundary chemistry and structure,” *MRS Bulletin*, vol. 46, no. 3, pp. 225–235, Mar. 2021, doi: 10.1557/s43577-021-00055-x.

[5] D. Raabe *et al.*, “Current Challenges and Opportunities in Microstructure-Related Properties of Advanced High-Strength Steels,” *Metallurgical and Materials Transactions A: Physical Metallurgy and Materials Science*, vol. 51, no. 11, pp. 5517–5586, Nov. 2020, doi: 10.1007/s11661-020-05947-2.

[6] E. D. Hondros and C. Lea, “Grain boundary microchemistry and stress-corrosion failure of mild steel,” *Nature*, vol. 289, no. 5799, pp. 663–665, 1981, doi: 10.1038/289663a0.

[7] D. E. Spearot and M. D. Sangid, “Insights on slip transmission at grain boundaries from atomistic simulations,” *Current Opinion in Solid State and Materials Science*, vol. 18, no. 4. Elsevier Ltd, pp. 188–195, Aug. 01, 2014. doi: 10.1016/j.cossms.2014.04.001.

[8] D. Brandon, “25 Year Perspective Defining grain boundaries: An historical perspective the development and limitations of coincident site lattice models,” *Materials Science and Technology*, vol. 26, no. 7. pp. 762–773, Jul. 01, 2010. doi: 10.1179/026708310X12635619987989.

[9] D. G. Brandon, “The structure of high-angle grain boundaries,” *Acta Metallurgica*, vol. 14, no. 11, pp. 1479–1484, 1966, doi: 10.1016/0001-6160(66)90168-4.

[10] E. D. Hondros, “Rule for surface enrichment in solutions,” *Scripta Metallurgica*, vol. 14, no. 3, pp. 345–348, 1980, doi: 10.1016/0036-9748(80)90357-9.

[11] A. P. Sutton, R. W. Balluffi, and V. Vitek, “On intrinsic secondary grain boundary dislocation arrays in high angle symmetrical tilt grain boundaries,” *Scripta Metallurgica*, vol. 15, no. 9, pp. 989–994, 1981, doi: 10.1016/0036-9748(81)90240-4.

[12] H. Grimmer, “Coincidence-site lattices,” *Acta Crystallographica Section A*, vol. 32, no. 5, pp. 783–785, Sep. 1976, doi: 10.1107/S056773947601231X.

[13] F. C. FRANK, “Grain Boundaries in Metals,” *Nature*, vol. 181, no. 4614, pp. 976–977, Apr. 1958, doi: 10.1038/181976b0.

[14] M. E. Glicksman and R. A. Masumura, “GRAIN BOUNDARY STRUCTURE AND ENERGETICS.,” *Metall Trans A*, vol. 8 A, no. 9, pp. 1373–1382, 1977, doi: 10.1007/BF02642851.

[15] V. Y. Gertsman, A. P. Zhilyaev, and J. A. Szpunar, “Grain boundary misorientation distributions in monoclinic zirconia,” *Modelling and Simulation in Materials Science and Engineering*, vol. 5, no. 1, pp. 35–52, Jan. 1997, doi: 10.1088/0965-0393/5/1/003.

[16] J. M. Howe, *Solid-Liquid and Solid-Solid Interfaces*. 1997. Accessed: Jun. 28, 2021. [Online]. Available: https://www.wiley.com/en-us/9780471138303

[17] F. Weinberg, “Grain boundaries in metals,” *Progress in Metal Physics*, vol. 8, no. C, pp. 105–146, Jan. 1959, doi: 10.1016/0502-8205(59)90014-0.

[18] D. Mclean and A. Maradudin, “Grain Boundaries in Metals,” *Citation: Physics Today*, vol. 11, p. 35, 1958, doi: 10.1063/1.3062658.

[19] Saha, M., 2022. Grain boundary segregation in steels: Towards engineering the design of internal interfaces. *arXiv preprint arXiv:2202.12971*.

[20] A. P. Sutton and R. W. Balluffi, “Overview no. 61 On geometric criteria for low interfacial energy,” *Acta Metallurgica*, vol. 35, no. 9, pp. 2177–2201, 1987, doi: 10.1016/0001-6160(87)90067-8.

[21] W. T. Read and W. Shockley, “Dislocation models of crystal grain boundaries,” *Physical Review*, vol. 78, no. 3, pp. 275–289, 1950, doi: 10.1103/PhysRev.78.275.

[22] J. W. Cahn, Y. Mishin, and A. Suzuki, “Duality of dislocation content of grain boundaries,” *Philosophical Magazine*, vol. 86, no. 25–26, pp. 3965–3980, Sep. 2006, doi: 10.1080/14786430500536909.

[23] A. H. Cottrell, “Unified theory of effects of segregated interstitials on grain boundary cohesion,” *Materials Science and Technology (United Kingdom)*, vol. 6, no. 9, pp. 806–810, 1990, doi: 10.1179/mst.1990.6.9.806.

[24] A. Kelly, W. R. Tyson, and A. H. Cottrell, “Ductile and brittle crystals,” *Philosophical Magazine*, vol. 15, no. 135, pp. 567–586, 1967, doi: 10.1080/14786436708220903.

[25] W. T. Geng, A. J. Freeman, and G. B. Olson, “Influence of alloying additions on the impurity induced grain boundary embrittlement,” *Solid State Communications*, vol. 119, no. 10–11, pp. 585–590, 2001, doi: 10.1016/S0038-1098(01)00298-8.

[26] W. T. Geng, A. J. Freeman, and G. B. Olson, “Influence of alloying additions on grain boundary cohesion of transition metals: First-principles determination and its phenomenological extension,” *Physical Review B - Condensed Matter and Materials Physics*, vol. 63, no. 16, pp. 1–9, 2001, doi: 10.1103/PhysRevB.63.165415.

[27] W. T. Geng, A. J. Freeman, R. Wu, and G. B. Olson, “Effect of Mo and Pd on the grain-boundary cohesion of Fe,” *Physical Review B - Condensed Matter and Materials Physics*, vol. 62, no. 10, pp. 6208–6214, 2000, doi: 10.1103/PhysRevB.62.6208.

[28] H. K. Birnbaum and P. Sofronis, “Hydrogen-enhanced localized plasticity-a mechanism for hydrogen-related fracture,” *Materials Science and Engineering A*, vol. 176, no. 1–2, pp. 191–202, Mar. 1994, doi: 10.1016/0921-5093(94)90975-X.

[29] B. A. Szost, R. H. Vegter, and P. E. J. Rivera-Díaz-Del-Castillo, “Hydrogen-trapping mechanisms in nanostructured steels,” *Metallurgical and Materials Transactions A: Physical Metallurgy and Materials Science*, vol. 44, no. 10, pp. 4542–4550, Oct. 2013, doi: 10.1007/s11661-013-1795-7.

[30] K. Takai, H. Shoda, H. Suzuki, and M. Nagumo, “Lattice defects dominating hydrogen-related failure of metals,” *Acta Materialia*, vol. 56, no. 18, pp. 5158–5167, Oct. 2008, doi: 10.1016/j.actamat.2008.06.031.

[31] Y. Toji, H. Matsuda, M. Herbig, P. P. Choi, and D. Raabe, “Atomic-scale analysis of carbon partitioning between martensite and austenite by atom probe tomography and correlative transmission electron microscopy,” *Acta Materialia*, vol. 65, pp. 215–228, Feb. 2014, doi: 10.1016/j.actamat.2013.10.064.

[32] T. Frolov and Y. Mishin, “Thermodynamics of coherent interfaces under mechanical stresses. II. Application to atomistic simulation of grain boundaries,” *Physical Review B - Condensed Matter and Materials Physics*, vol. 85, no. 22, 2012, doi: 10.1103/PhysRevB.85.224107.

[33] Z. T. Trautt and Y. Mishin, “Grain boundary migration and grain rotation studied by molecular dynamics,” *Acta Materialia*, vol. 60, no. 5, pp. 2407–2424, 2012, doi: 10.1016/j.actamat.2012.01.008.

[34] M. Winning and A. D. Rollett, “Transition between low and high angle grain boundaries,” *Acta Materialia*, vol. 53, no. 10, pp. 2901–2907, Jun. 2005, doi: 10.1016/j.actamat.2005.03.005.

[35] A. D. Rollett and P. N. Kalu, “Grain Boundary Properties : Energy,” *Revue de Métallurgie*, pp. 1–82, 2008.

[36] A. D. Rollett, D. J. Srolovitz, and A. Karma, “Editorial: Microstructural evolution based on fundamental interracial properties,” *Interface Science*, vol. 10, no. 2–3. p. 119, Jul. 2002. doi: 10.1023/A:1015809611353.

[37] S. Mandal, B. T. Gockel, and A. D. Rollett, “Application of canonical correlation analysis to a sensitivity study of constitutive model parameter fitting,” *Materials and Design*, vol. 132, pp. 30–43, Oct. 2017, doi: 10.1016/j.matdes.2017.06.050.

[38] N. Bandyopadhyay, C. L. Briant, and E. L. Hall, “Carbide precipitation, grain boundary segregation, and temper embrittlement in NiCrMoV rotor steels,” *Metallurgical Transactions A 1985 16:5*, vol. 16, no. 5, pp. 721–737, May 1985, doi: 10.1007/BF02814824.

[39] C. L. Brunt, “Sources of variability in grain boundary segregation,” *Acta Metallurgica*, vol. 31, no. 2, pp. 257–266, Feb. 1983, doi: 10.1016/0001-6160(83)90102-5.

[40] G. M. Carinci, “Grain boundary segregation of boron in an austenitic stainless steel,” *Applied Surface Science*, vol. 76–77, no. C, pp. 266–271, Mar. 1994, doi: 10.1016/0169-4332(94)90353-0.

[41] S. H. Song, J. Wu, L. Q. Weng, and Z. X. Yuan, “Fractographic changes caused by phosphorus grain boundary segregation for a low alloy structural steel,” *Materials Science and Engineering: A*, vol. 497, no. 1–2, pp. 524–527, Dec. 2008, doi: 10.1016/J.MSEA.2008.07.036.

[42] X. M. Chen, S. H. Song, L. Q. Weng, and S. J. Liu, “Solute grain boundary segregation during high temperature plastic deformation in a Cr–Mo low alloy steel,” *Materials Science and Engineering: A*, vol. 528, no. 25–26, pp. 7663–7668, Sep. 2011, doi: 10.1016/J.MSEA.2011.06.084.

[43] C. L. Briant and S. K. Banerji, “Intergranular failure in steel: the role of grain-boundary composition,” *International Materials Reviews*, vol. 23, no. 1, pp. 164–199, Jan. 2012, doi: 10.1179/095066078790136652.

[44] X. Tingdong, “Non-equilibrium grain-boundary segregation kinetics,” *Journal of Materials Science 1987 22:1*, vol. 22, no. 1, pp. 337–345, Jan. 1987, doi: 10.1007/BF01160590.

[45] T. Xu and S. Song, “A kinetic model of non-equilibrium grain-boundary segregation,” *Acta Metallurgica*, vol. 37, no. 9, pp. 2499–2506, Sep. 1989, doi: 10.1016/0001-6160(89)90048-5.

[46] X. Sauvage, A. Ganeev, Y. Ivanisenko, N. Enikeev, M. Murashkin, and R. Valiev, “Grain Boundary Segregation in UFG Alloys Processed by Severe Plastic Deformation,” *Advanced Engineering Materials*, vol. 14, no. 11, pp. 968–974, Nov. 2012, doi: 10.1002/ADEM.201200060.

[47] M. P. Seah, “Segregation and the Strength of Grain Boundaries.,” *Proc R Soc Lond Ser A*, vol. 349, no. 1659, pp. 535–554, 1976, doi: 10.1098/rspa.1976.0088.

[48] M. P. Seah, “Adsorption-induced interface decohesion,” *Acta Metallurgica*, vol. 28, no. 7, pp. 955–962, Jul. 1980, doi: 10.1016/0001-6160(80)90112-1.

[49] D. Raabe *et al.*, “Metallic composites processed via extreme deformation: Toward the limits of strength in bulk materials,” *MRS Bulletin*, vol. 35, no. 12, pp. 982–991, Jan. 2010, doi: 10.1557/mrs2010.703.

[50] P. Lejček, “Effect of Variables on Equilibrium Grain Boundary Segregation,” in *Springer Series in Materials Science*, 2010. doi: 10.1007/978-3-642-12505-8_5.

[51] Y. Ohmori and T. Kunitake, “Effects of austenite grain size and grain boundary segregation of impurity atoms on high temperature ductility,” *Metal Science*, vol. 17, no. 7, pp. 325–332, Jul. 1983, doi: 10.1179/030634583790420781.

[52] P. Lejček, “On the thermodynamic description of grain boundary segregation in polycrystals,” *Materials Science and Engineering A*, vol. 185, no. 1–2, pp. 109–114, Sep. 1994, doi: 10.1016/0921-5093(94)90933-4.

[53] L. Karlsson and H. Nordén, “Overview no. 63 Non-equilibrium grain boundary segregation of boron in austenitic stainless steel-II. Fine scale segregation behaviour,” *Acta Metallurgica*, vol. 36, no. 1, pp. 13–24, Jan. 1988, doi: 10.1016/0001-6160(88)90024-7.

[54] S. H. Song, H. Zhuang, J. Wu, L. Q. Weng, Z. X. Yuan, and T. H. Xi, “Dependence of ductile-to-brittle transition temperature on phosphorus grain boundary segregation for a 2.25Cr1Mo steel,” *Materials Science and Engineering: A*, vol. 486, no. 1–2, pp. 433–438, Jul. 2008, doi: 10.1016/J.MSEA.2007.09.032.

[55] M. A. Tschopp and D. L. McDowell, “Structures and energies of ∑3 asymmetric tilt grain boundaries in copper and aluminium,” *Philosophical Magazine*, vol. 87, no. 22, pp. 3147–3173, Aug. 2007, doi: 10.1080/14786430701255895.

[56] M. A. Tschopp, K. N. Solanki, F. Gao, X. Sun, M. A. Khaleel, and M. F. Horstemeyer, “Probing grain boundary sink strength at the nanoscale: Energetics and length scales of vacancy and interstitial absorption by grain boundaries in α-Fe,” *Physical Review B - Condensed Matter and Materials Physics*, vol. 85, no. 6, Feb. 2012, doi: 10.1103/PhysRevB.85.064108.

[57] M. A. V. Chapman and R. G. Faulkner, “Computer modelling of grain boundary segregation,” *Acta Metallurgica*, vol. 31, no. 5, pp. 677–689, May 1983, doi: 10.1016/0001-6160(83)90083-4.

[58] B. W. Krakauer and D. N. Seidman, “Absolute atomic-scale measurements of the Gibbsian interfacial excess of solute at internal interfaces,” *Physical Review B*, vol. 48, no. 9, pp. 6724–6727, 1993, doi: 10.1103/PhysRevB.48.6724.

[59] E. D. Hondros and D. McLean, “Cohesion margin of copper,” *Philosophical Magazine*, vol. 29, no. 4, pp. 771–795, 1974, doi: 10.1080/14786437408222070.

[60] I. Langmuir, “The adsorption of gases on plane surfaces of glass, mica and platinum,” *Journal of the American Chemical Society*, vol. 40, no. 9, pp. 1361–1403, Sep. 1918, doi: 10.1021/ja02242a004.

[61] P. Lejček, M. Šob, V. Paidar, and V. Vitek, “Why calculated energies of grain boundary segregation are unreliable when segregant solubility is low,” *Scripta Materialia*, vol. 68, no. 8, pp. 547–550, Apr. 2013, doi: 10.1016/j.scriptamat.2012.11.019.

[62] P. Lejček and S. Hofmann, “Entropy-dominated grain boundary segregation,” *Journal of Materials Science*, vol. 56, no. 12, pp. 7464–7473, Apr. 2021, doi: 10.1007/s10853-021-05800-w.

[63] P. Lejček, S. Hofmann, M. Všianská, and M. Šob, “Entropy matters in grain boundary segregation,” *Acta Materialia*, vol. 206, p. 116597, Mar. 2021, doi: 10.1016/j.actamat.2020.116597.

[64] R. H. Ewing, “An analytical approach to interfacial entropy,” *Acta Metallurgica*, vol. 19, no. 12, pp. 1359–1362, 1971, doi: 10.1016/0001-6160(71)90073-3.

[65] P. Lejček and S. Hofmann, “Thermodynamics and structural aspects of grain boundary segregation,” *Critical Reviews in Solid State and Materials Sciences*, vol. 20, no. 1, pp. 1–85, 1995, doi: 10.1080/10408439508243544.

[66] P. Lejček and S. Hofmann, “Grain boundary segregation diagrams of α-iron,” *Interface Science*, vol. 1, no. 2, pp. 163–174, 1993, doi: 10.1007/BF00203606.

[67] P. Lejcek and S. Hofmann, “Thermodynamics of grain boundary segregation and applications to anisotropy, compensation effect and prediction,” *Critical Reviews in Solid State and Materials Sciences*, vol. 33, no. 2, pp. 133–163, Apr. 2008, doi: 10.1080/10408430801907649.

[68] P. Lejček, S. Hofmann, and V. Paidar, “The significance of entropy in grain boundary segregation,” *Materials*, vol. 12, no. 3, pp. 1–9, 2019, doi: 10.3390/ma12030492.

[69] P. Lejček, “Enthalpy-entropy compensation effect in grain boundary phenomena,” *Zeitschrift fuer Metallkunde/Materials Research and Advanced Techniques*, vol. 96, no. 10, pp. 1129–1133, 2005, doi: 10.3139/146.101151.

[70] P. Lejček, “Characterization of grain boundary segregation in an Fe-Si alloy,” *Analytica Chimica Acta*, vol. 297, no. 1–2, pp. 165–178, Oct. 1994, doi: 10.1016/0003-2670(93)E0388-N.

[71] P. Lejček, R. Konečná, and J. Janovec, “Solute segregation to ferrite grain boundaries in nodular cast iron: Experiment and prediction,” *Surface and Interface Analysis*, vol. 40, no. 3–4, pp. 503–506, 2008, doi: 10.1002/sia.2659.

[72] P. Lejček, M. Všianská, and M. Šob, “Recent trends and open questions in grain boundary segregation,” *Journal of Materials Research*, vol. 33, no. 18, pp. 2647–2660, Sep. 2018, doi: 10.1557/jmr.2018.230.

[73] P. Lejček, J. Adámek, and S. Hofmann, “Anisotropy of grain boundary segregation in $\Sigma = 5$ bicrystals of α-iron,” *Surface Science*, vol. 264, no. 3, pp. 449–454, Mar. 1992, doi: 10.1016/0039-6028(92)90201-G.

[74] P. Lejček, S. Hofmann, and J. Janovec, “Prediction of enthalpy and entropy of solute segregation at individual grain boundaries of α-iron and ferrite steels,” *Materials Science and Engineering A*, vol. 462, no. 1–2, pp. 76–85, Jul. 2007, doi: 10.1016/j.msea.2006.02.463.

[75] P. Lejček, M. Šob, and V. Paidar, “Interfacial segregation and grain boundary embrittlement: An overview and critical assessment of experimental data and calculated results,” *Progress in Materials Science*, vol. 87. 2017. doi: 10.1016/j.pmatsci.2016.11.001.

[76] S. Hofmann and P. Lejček, “Correlation between segregation enthalpy, solid solubility and interplanar spacing of Σ=5 tilt grain boundaries in α-iron,” *Scripta Metallurgica et Materiala*, vol. 25, no. 10, pp. 2259–2262, 1991, doi: 10.1016/0956-716X(91)90011-O.

[77] P. Lejček and S. Hofmann, “Grain boundary segregation diagrams of α-iron,” *Interface Science*, vol. 1, no. 2, pp. 163–174, 1993, doi: 10.1007/BF00203606.

[78] M. Guttmann, “Interfacial Segregation in Multicomponent Systems,” in *Atomistics of Fracture*, Boston, MA: Springer US, 1983, pp. 465–494. doi: 10.1007/978-1-4613-3500-9_17.

[79] M. Guttmann, “Grain boundary segregation, two dimensional compound formation, and precipitation,” *Metallurgical Transactions A*, vol. 8, no. 9, pp. 1383–1401, Sep. 1977, doi: 10.1007/BF02642852.

[80] M. Guttmann, “Equilibrium segregation in a ternary solution: A model for temper embrittlement,” *Surface Science*, vol. 53, no. 1, pp. 213–227, 1975, doi: 10.1016/0039-6028(75)90125-9.

[81] M. Guttmann, “Interfacial Segregation in Multicomponent Systems,” in *Atomistics of Fracture*, Boston, MA: Springer US, 1983, pp. 465–494. doi: 10.1007/978-1-4613-3500-9_17.

[82] P. Wynblatt and D. Chatain, “Anisotropy of segregation at grain boundaries and surfaces,” *Metallurgical and Materials Transactions A: Physical Metallurgy and Materials Science*, vol. 37, no. 9. pp. 2595–2620, Sep. 2006. doi: 10.1007/BF02586096.

[83] M. Daly *et al.*, “A multi-scale correlative investigation of ductile fracture,” *Acta Materialia*, vol. 130, pp. 56–68, May 2017, doi: 10.1016/j.actamat.2017.03.028.

[84] S. E. Hopkin, M. Danaie, G. Guetard, P. Rivera-Diaz-del-Castillo, P. A. J. Bagot, and M. P. Moody, “Correlative atomic scale characterisation of secondary carbides in M50 bearing steel,” *Philosophical Magazine*, vol. 98, no. 9, pp. 766–782, Mar. 2018, doi: 10.1080/14786435.2017.1410290.

[85] T. Schwarz, G. Stechmann, B. Gault, O. Cojocaru-Mirédin, R. Wuerz, and D. Raabe, “Correlative transmission Kikuchi diffraction and atom probe tomography study of Cu(In,Ga)Se2 grain boundaries,” *Progress in Photovoltaics: Research and Applications*, vol. 26, no. 3, pp. 196–204, Mar. 2018, doi: 10.1002/pip.2966.

[86] M. Herbig, D. Raabe, Y. J. Li, P. Choi, S. Zaefferer, and S. Goto, “Atomic-Scale Quantification of Grain Boundary Segregation in Nanocrystalline Material,” *APS*, vol. 112, no. 12, Dec. 2014, doi: 10.1103/PhysRevLett.112.126103.

[87] Y. J. Li, A. Kostka, A. Savan, and A. Ludwig, “Correlative chemical and structural investigations of accelerated phase evolution in a nanocrystalline high entropy alloy,” *Scripta Materialia*, vol. 183, pp. 122–126, Jul. 2020, doi: 10.1016/j.scriptamat.2020.03.016.

[88] L. Yao, S. P. Ringer, J. M. Cairney, and M. K. Miller, “The anatomy of grain boundaries: Their structure and atomic-level solute distribution,” *Scripta Materialia*, vol. 69, no. 8, pp. 622–625, Oct. 2013, doi: 10.1016/j.scriptamat.2013.07.013.

[89] B. Gault, M. P. Moody, J. M. Cairney, and S. P. Ringer, “Atom Atom probe probe crystallography,” *Materials Today*, vol. 15, no. 9, pp. 378–386, 2012, doi: 10.1016/S1369-7021(12)70164-5.

[90] B. Gault, M. P. Moody, J. M. Cairney, and S. P. Ringer, “Specimen Preparation,” in *Springer Series in Materials Science*, vol. 160, Springer Science and Business Media Deutschland GmbH, 2012, pp. 71–110. doi: 10.1007/978-1-4614-3436-8_4.

[91] D. J. Larson, B. P. Geiser, T. J. Prosa, and T. F. Kelly, “Atom Probe Tomography Spatial Reconstruction : Current Status and Future Directions,” *Current Opinion in Solid State and Materials Science*, vol. 39, pp. 740–741, 2012.

[92] A. v. Ceguerra *et al.*, “The rise of computational techniques in atom probe microscopy,” *Current Opinion in Solid State and Materials Science*. 2013. doi: 10.1016/j.cossms.2013.09.006.

[93] O. Dmitrieva *et al.*, “Chemical gradients across phase boundaries between martensite and austenite in steel studied by atom probe tomography and simulation,” *Acta Materialia*, vol. 59, no. 1, pp. 364–374, Jan. 2011, doi: 10.1016/j.actamat.2010.09.042.

[94] H. J. Grabke, R. Möller, H. Erhart, and S. S. Brenner, “Effects of the alloying elements Ti, Nb, Mo and V on the grain boundary segregation of P in iron and steels,” *Surface and Interface Analysis*, vol. 10, no. 4, pp. 202–209, Apr. 1987, doi: 10.1002/sia.740100405.

[95] F. Christien, R. le Gall, and G. Saindrenan, “Phosphorus grain boundary segregation in steel 17-4PH,” *Scripta Materialia*, vol. 48, no. 1, pp. 11–16, Jan. 2003, doi: 10.1016/S1359-6462(02)00309-3.

[96] J. Takahashi, K. Kawakami, K. Ushioda, S. Takaki, N. Nakata, and T. Tsuchiyama, “Quantitative analysis of grain boundaries in carbon- and nitrogen-added ferritic steels by atom probe tomography,” *Scripta Materialia*, vol. 66, no. 5, pp. 207–210, Mar. 2012, doi: 10.1016/j.scriptamat.2011.10.026.

[97] G. da Rosa *et al.*, “Grain-boundary segregation of boron in high-strength steel studied by nano-SIMS and atom probe tomography,” *Acta Materialia*, vol. 182, pp. 226–234, Jan. 2020, doi: 10.1016/j.actamat.2019.10.029.

[98] Z. N. Abdellah, R. Chegroune, M. Keddam, B. Bouarour, L. Haddour, and A. Elias, “The phase stability in the Fe-B binary system: Comparison between the interstitial and substitutional models,” *Defect and Diffusion Forum*, vol. 322, pp. 1–9, Mar. 2012, doi: 10.4028/www.scientific.net/DDF.322.1.

[99] J. MORRAL, M. JE, and J. W. JR, “THE BINDING ENERGY OF BORON TO AUSTENITE GRAIN BOUNDARIES AS CALCULATED FROM AUTORADIOGRAPHY,” *THE BINDING ENERGY OF BORON TO AUSTENITE GRAIN BOUNDARIES AS CALCULATED FROM AUTORADIOGRAPHY*, 1980.

[100] R. G. Faulkner, “Radiation-induced grain boundary segregation in nuclear reactor steels,” *Journal of Nuclear Materials*, vol. 251, pp. 269–275, 1997, doi: 10.1016/S0022-3115(97)00248-1.

[101] S. v. Fedotova, E. A. Kuleshova, D. A. Maltsev, and M. A. Saltykov, “Complex study of grain boundary segregation in long-term irradiated reactor pressure vessel steels,” *Journal of Nuclear Materials*, vol. 528, p. 151865, Jan. 2020, doi: 10.1016/j.jnucmat.2019.151865.

[102] K. Hata, H. Takamizawa, T. Hojo, K. Ebihara, Y. Nishiyama, and Y. Nagai, “Grain-boundary phosphorus segregation in highly neutron-irradiated reactor pressure vessel steels and its effect on irradiation embrittlement,” *Journal of Nuclear Materials*, vol. 543, p. 152564, Jan. 2021, doi: 10.1016/j.jnucmat.2020.152564.

[103] T. Toyama *et al.*, “Grain boundary segregation in neutron-irradiated 304 stainless steel studied by atom probe tomography,” in *Journal of Nuclear Materials*, Jun. 2012, vol. 425, no. 1–3, pp. 71–75. doi: 10.1016/j.jnucmat.2011.11.072.

[104] E. A. Kenik, T. Inazumi, and G. E. C. Bell, “Radiation-induced grain boundary segregation and sensitization of a neutron-irradiated austenitic stainless steel,” *Journal of Nuclear Materials*, vol. 183, no. 3, pp. 145–153, Aug. 1991, doi: 10.1016/0022-3115(91)90482-M.

[105] G. Shigesato, T. Fujishiro, and T. Hara, “Boron segregation to austenite grain boundary in low alloy steel measured by aberration corrected STEM-EELS,” *Materials Science and Engineering A*, vol. 556, pp. 358–365, Oct. 2012, doi: 10.1016/j.msea.2012.06.099.

[106] Y. Ma *et al.*, “Phase boundary segregation-induced strengthening and discontinuous yielding in ultrafine-grained duplex medium-Mn steels,” *Acta Materialia*, vol. 200, pp. 389–403, Nov. 2020, doi: 10.1016/j.actamat.2020.09.007.

[107] T. Frolov, “Effect of interfacial structural phase transitions on the coupled motion of grain boundaries: A molecular dynamics study,” *Applied Physics Letters*, vol. 104, no. 21, p. 211905, May 2014, doi: 10.1063/1.4880715.

[108] G. Gottstein, L. S. Shvindlerman, and B. Zhao, “Thermodynamics and kinetics of grain boundary triple junctions in metals: Recent developments,” *Scripta Materialia*, vol. 62, no. 12, pp. 914–917, 2010, doi: 10.1016/j.scriptamat.2010.03.017.

[109] G. Gottstein, D. A. Molodov, and L. S. Shvindlerman, “Grain boundary migration in metals: recent developments,” *Interface Science*, vol. 6, no. 1–2, pp. 7–22, Feb. 1998, doi: 10.1023/A:1008641617937.

[110] M. M. Abramova *et al.*, “Grain boundary segregation induced strengthening of an ultrafine-grained austenitic stainless steel,” *Materials Letters*, vol. 136, pp. 349–352, Dec. 2014, doi: 10.1016/j.matlet.2014.07.188.

[111] J. C. Han, J. B. Seol, M. Jafari, J. E. Kim, S. J. Seo, and C. G. Park, “Competitive grain boundary segregation of phosphorus and carbon governs delamination crack in a ferritic steel,” *Materials Characterization*, vol. 145, pp. 454–460, Nov. 2018, doi: 10.1016/j.matchar.2018.08.060.

[112] M. Kuzmina, D. Ponge, and D. Raabe, “Grain boundary segregation engineering and austenite reversion turn embrittlement into toughness: Example of a 9 wt.% medium Mn steel,” *Acta Materialia*, vol. 86, pp. 182–192, Mar. 2015, doi: 10.1016/j.actamat.2014.12.021.

[113] J. T. Benzing *et al.*, “Multi-scale characterization of austenite reversion and martensite recovery in a cold-rolled medium-Mn steel,” *Acta Materialia*, vol. 166, pp. 512–530, Mar. 2019, doi: 10.1016/j.actamat.2019.01.003.

[114] A. M. Ravi, A. Kumar, M. Herbig, J. Sietsma, and M. J. Santofimia, “Impact of austenite grain boundaries and ferrite nucleation on bainite formation in steels,” *Acta Materialia*, vol. 188, pp. 424–434, Apr. 2020, doi: 10.1016/j.actamat.2020.01.065.

[115] M. Herbig *et al.*, “Grain boundary segregation in Fe-Mn-C twinning-induced plasticity steels studied by correlative electron backscatter diffraction and atom probe tomography,” *Acta Materialia*, vol. 83, pp. 37–47, Jan. 2015, doi: 10.1016/j.actamat.2014.09.041.

[116] S. Araki, K. Mashima, T. Masumura, T. Tsuchiyama, S. Takaki, and T. Ohmura, “Effect of grain boundary segregation of carbon on critical grain boundary strength of ferritic steel,” *Scripta Materialia*, vol. 169, pp. 38–41, Aug. 2019, doi: 10.1016/j.scriptamat.2019.05.001.

[117] L. Yuan, D. Ponge, J. Wittig, P. Choi, J. A. Jiménez, and D. Raabe, “Nanoscale austenite reversion through partitioning, segregation and kinetic freezing: Example of a ductile 2 GPa Fe-Cr-C steel,” *Acta Materialia*, vol. 60, no. 6–7, pp. 2790–2804, Apr. 2012, doi: 10.1016/j.actamat.2012.01.045.

[118] Y. J. Li *et al.*, “Atomic-scale mechanisms of deformation-induced cementite decomposition in pearlite,” *Acta Materialia*, vol. 59, no. 10, pp. 3965–3977, Jun. 2011, doi: 10.1016/j.actamat.2011.03.022.

[119] Y. J. Li, P. Choi, S. Goto, C. Borchers, D. Raabe, and R. Kirchheim, “Evolution of strength and microstructure during annealing of heavily cold-drawn 6.3 GPa hypereutectoid pearlitic steel wire,” *Acta Materialia*, vol. 60, no. 9, pp. 4005–4016, May 2012, doi: 10.1016/j.actamat.2012.03.006.

[120] Y. J. Lia *et al.*, “Atom probe tomography characterization of heavily cold drawn pearlitic steel wire,” *Ultramicroscopy*, vol. 111, no. 6, pp. 628–632, May 2011, doi: 10.1016/j.ultramic.2010.11.010.

[121] Y. S. Chen *et al.*, “Direct observation of individual hydrogen atoms at trapping sites in a ferritic steel,” *Science*, vol. 355, no. 6330, pp. 1196–1199, Mar. 2017, doi: 10.1126/science.aal2418.

[122] J. Cairney, “Atoms on the move - Finding the hydrogen,” *Science*, vol. 355, no. 6330. American Association for the Advancement of Science, pp. 1128–1129, Mar. 17, 2017. doi: 10.1126/science.aam8616.

[123] I. M. Robertson *et al.*, “Hydrogen Embrittlement Understood,” *Metallurgical and Materials Transactions B: Process Metallurgy and Materials Processing Science*, vol. 46, no. 3, pp. 1085–1103, Jun. 2015, doi: 10.1007/s11663-015-0325-y.

[124] Y. S. Chen *et al.*, “Observation of hydrogen trapping at dislocations, grain boundaries, and precipitates,” *Science*, vol. 367, no. 6474, pp. 171–175, Jan. 2020, doi: 10.1126/science.aaz0122.

[125] M. Koyama, E. Akiyama, and K. Tsuzaki, “Effect of hydrogen content on the embrittlement in a Fe-Mn-C twinning-induced plasticity steel,” *Corrosion Science*, vol. 59, pp. 277–281, Jun. 2012, doi: 10.1016/j.corsci.2012.03.009.

[126] I. R. Souza Filho *et al.*, “Sustainable steel through hydrogen plasma reduction of iron ore: Process, kinetics, microstructure, chemistry,” *Acta Materialia*, vol. 213, p. 116971, Jul. 2021, doi: 10.1016/j.actamat.2021.116971.

[127] S. H. Kim *et al.*, “Influence of microstructure and atomic-scale chemistry on the direct reduction of iron ore with hydrogen at 700°C,” *Acta Materialia*, vol. 212, p. 116933, Jun. 2021, doi: 10.1016/j.actamat.2021.116933.

[128] D. Raabe, C. C. Tasan, and E. A. Olivetti, “Strategies for improving the sustainability of structural metals,” *Nature*, vol. 575, no. 7781. Nature Publishing Group, pp. 64–74, Nov. 07, 2019. doi: 10.1038/s41586-019-1702-5.

[129] M. P. Phaniraj, H. J. Kim, J. Y. Suh, J. H. Shim, S. J. Park, and T. H. Lee, “Hydrogen embrittlement in high interstitial alloyed 18Cr10Mn austenitic stainless steels,” *International Journal of Hydrogen Energy*, vol. 40, no. 39, pp. 13635–13642, Oct. 2015, doi: 10.1016/j.ijhydene.2015.07.163.

[130] D. Raabe, D. Ponge, O. Dmitrieva, and B. Sander, “Nanoprecipitate-hardened 1.5 GPa steels with unexpected high ductility,” *Scripta Materialia*, vol. 60, no. 12, pp. 1141–1144, Jun. 2009, doi: 10.1016/j.scriptamat.2009.02.062.

[131] B. C. Cameron, M. Koyama, and C. C. Tasan, “Phase Stability Effects on Hydrogen Embrittlement Resistance in Martensite–Reverted Austenite Steels,” *Metallurgical and Materials Transactions A: Physical Metallurgy and Materials Science*, vol. 50, no. 1, pp. 29–34, Jan. 2019, doi: 10.1007/s11661-018-4948-x.

[132] Y. S. Chun, J. S. Kim, K. T. Park, Y. K. Lee, and C. S. Lee, “Role of e{open} martensite in tensile properties and hydrogen degradation of high-Mn steels,” *Materials Science and Engineering A*, vol. 533, pp. 87–95, Jan. 2012, doi: 10.1016/j.msea.2011.11.039.

[133] D. Raabe, D. Ponge, O. Dmitrieva, and B. Sander, “Designing ultrahigh strength steels with good ductility by combining transformation induced plasticity and martensite aging,” *Advanced Engineering Materials*, vol. 11, no. 7, pp. 547–555, Jul. 2009, doi: 10.1002/adem.200900061.

[134] G. B. Olson and M. Cohen, “A mechanism for the strain-induced nucleation of martensitic transformations,” *Journal of The Less-Common Metals*, vol. 28, no. 1, pp. 107–118, 1972, doi: 10.1016/0022-5088(72)90173-7.

[135] N. Nakada, T. Tsuchiyama, S. Takaki, and S. Hashizume, “Variant selection of reversed austenite in lath martensite,” *ISIJ International*, vol. 47, no. 10, pp. 1527–1532, 2007, doi: 10.2355/isijinternational.47.1527.

[136] M. R. Hickson, P. J. Hurley, R. K. Gibbs, G. L. Kelly, and P. D. Hodgson, “The Production of Ultrafine Ferrite in Low-Carbon Steel by Strain-Induced Transformation.”

[137] G. Krauss, “Martensite in steel: Strength and structure,” *Materials Science and Engineering A*, vol. 273–275, pp. 40–57, Dec. 1999, doi: 10.1016/s0921-5093(99)00288-9.

[138] D. J. Rowenhorst, A. Gupta, C. R. Feng, and G. Spanos, “3D Crystallographic and morphological analysis of coarse martensite: Combining EBSD and serial sectioning,” *Scripta Materialia*, vol. 55, no. 1, pp. 11–16, Jul. 2006, doi: 10.1016/J.SCRIPTAMAT.2005.12.061.

[139] M. Calcagnotto, D. Ponge, E. Demir, and D. Raabe, “Orientation gradients and geometrically necessary dislocations in ultrafine grained dual-phase steels studied by 2D and 3D EBSD,” *Materials Science and Engineering: A*, vol. 527, no. 10–11, pp. 2738–2746, Apr. 2010, doi: 10.1016/J.MSEA.2010.01.004.